Cleaner Engineering and Technology 6 (2022) 100383

Contents lists available at ScienceDirect

Cleaner Engineering and Technology

journal homepage: www.sciencedirect.com/journal/cleaner-engineering-and-technology

Engineering performance of metakaolin based concrete

Deveshan L. Pillay [a], Oladimeji B. Olalusi [a,*], Moses W. Kiliswa [a], Paul O. Awoyera [b], John Temitope Kolawole [c,d], Adewumi John Babafemi [e]

[a] Department of Civil Engineering, Structural Engineering & Computational Mechanics Group (SECM), University of KwaZulu-Natal, Durban, South Africa
[b] Department of Civil Engineering, Covenant University, Ota, Nigeria
[c] Department of Building, Obafemi Awolowo University, Ile-Ife, Nigeria
[d] School of Architecture, Building and Civil Engineering, Loughborough University, UK
[e] Department of Civil Engineering, Stellenbosch University, South Africa

ARTICLE INFO

Keywords:
Supplementary cementitious materials
Chloride attack
Metakaolin
Engineering properties
Marine structures

ABSTRACT

The sustainable development goal (SDG) 14 of the 2030 Agenda for Sustainable Development aims at protection, conservation, and management of coastal ecosystems and resources, including by strengthening their resilience, to avoid significant adverse impacts. Coastal/marine structures are exposed to aggressive environmental conditions, such as chloride laden environment. Deterioration of reinforced concrete structures located in a coastal/marine setting can influence the safety, economic and sustainability aspects of the society. Hence, there is an increased need for sustainable materials with the ability to reduce the effects of chloride attack in concrete. This experimental study aims to investigate the engineering properties of metakaolin (MK) based concrete exposed to chloride attack. The investigation was conducted for different w/b ratios of 0.54–0.61. The MK, utilised as cementitious material, was varied from 0 to 20% with an increment of 5% and ages of concrete from 7 to 56 days were considered. The effects of the above-mentioned parameters on the various properties of concrete such as workability, compressive and flexural strength, durability, resistance to chloride attack and microstructure properties of the concrete samples were investigated. From the favourable strength and durability results that were observed during the experimental study (optimum compressive strength of 49.8 MPa for 10% MK and optimum flexural strength of 8.35 MPa for 5% MK), it can be concluded that MK is a feasible supplementary cementitious material for combatting chloride attack in coastal/marine concrete structures. The obtained results, in combination with the lack of carbon dioxide CO_2 released during the MK manufacturing process, further highlights the positive influence of MK on improving the serviceability and sustainability states of coastal/marine structures.

1. Introduction

Reinforced concrete (RC) remains an extensively used construction material due to its apparent benefits, some of which includes good strength, resilience, fire resistance, freeze-thaw resistance, chemical resistance, durability performance and versatility (Broomfield, 2007). It is a composite material made of steel and concrete. Concrete, in itself, is a heterogeneous material made of cement and aggregates with different shapes and sizes. Tamanna et al. (2020) estimated that more than 1 m^3 of concrete is produced per individual per year on a global scale. According to Tamanna et al. (2020), the cement manufacturing industry accounts for between 5 and 7% of the total worldwide carbon dioxide (CO_2) emissions. This has been further documented in Schneider (2019). On a global scale, the annual cement production for 2020 is projected to be approximately 5.9 billion tons, which results in 4.8 billion tons of CO_2 that will be produced (Singh and Middendorf, 2020). Harmful greenhouse gases, such as sulphur trioxide (SO_3) and nitrogen oxides (NO_X), are also byproducts of the cement manufacturing process and can also have an adverse impact on the environment. Large quantities of energy and raw materials are also consumed during the cement production process. The growing demand for future development can be attributed to the ever-expanding population and physical attributes that are experienced both locally and globally. It is expected that most of these developments will occur in marine and coastal regions, due to the fair trade and transport prospects, suitable locations for human settlements and ease of access linked with these areas (Alexander, 2016).

* Corresponding author.
E-mail address: olalusio@ukzn.ac.za (O.B. Olalusi).

https://doi.org/10.1016/j.clet.2021.100383
Received 30 April 2021; Received in revised form 13 December 2021; Accepted 25 December 2021
Available online 28 December 2021

However, several critical issues are affecting the structural and aesthetic performance of RC structures. Some of these factors are poor design and construction procedures, poor materials selection and exposure to aggressive environmental conditions, such as chloride laden environment (Broomfield, 2007). Khan et al. (2017) reported that the deterioration and failure of reinforced concrete structures located in coastal/marine areas could have a significant impact on the safety, economy and the sustainability aspect of the society. Chloride attack is the main factor affecting the durability performance of reinforced concrete structures located in coastal and marine environments (Tadayon et al., 2016). Chloride ingress also has a critical influence on the physical and chemical processes associated with the deterioration of the concrete microstructure and corrosion of the steel rebar (Chalee et al., 2009). The corrosion process commences when a critical concentration of chloride ions accumulates at the steel reinforcement (Aguirre-Guerrero et al., 2018). The propagation of chloride attack is initiated by the expansion/contraction and hydration/dehydration cycles, which leads to the development of cracks, spalling and reduction of load-bearing capacity in reinforced concrete structures (Khan et al., 2017). The cycles are directly influenced by changes in temperature and humidity, in chloride laden environments. Ultimately, this can lead to unsafe coastal/marine concrete structures with reduced service life. The economic loss due to premature failure and the cost of repairs can be very severe. In this context, it is of high importance to produce durable concrete structures with longer service life and less damage due to unforeseeable reasons.

Past research studies conducted by Owens (2013), Maes et al. (2012) and Song et al. (2008) have extensively analysed the durability problems resulting from chloride attack in concrete containing recycled materials and secondary products. From a marine and coastal engineering perspective, there is an increased need for alternate binder systems with the ability to reduce the penetration of chloride ions. Alternate binder materials are usually incorporated in concrete to enhance the fresh state, mechanical and durability performance of concrete exposed to chloride laden environments. Numerous research studies have extensively documented the positive impact of alternative binder systems, such as Metakaolin (MK), ground granulated blast furnace slag (GGBS), fly ash (FA), condensed silica fume (CSF), for partial replacement of cement. Some of these impacts include reduced heat of hydration (Maes et al., 2012), enhanced durability performance (Song et al., 2008) and improved concrete's resistance to chloride attack (Ayub et al., 2013).

Metakaolin (MK), unlike other supplementary cementitious materials such as granulated blast furnace slag (GGBS) and fly ash (FA), is a highly reactive pozzolanic material that exhibits more favourable concrete performance characteristics. Metakaolin ($(Al_2Si_2O_5)$ or AS_2) is produced via the process of hydroxylation, whereby kaolin ($(Al_2Si_2O_5(OH)_4)$ or AS_2H_4), which is a natural clay mineral, is heated to a temperature between 650 °C and 800 °C (Khatib, 2016). MK is an aluminosilicate material that is made up of varying amounts of alumina (40%–45%) and silica (50%–55%) (Khatib, 2016). It is typically a white powder with a particle diameter of approximately 2 μm, which is much finer than PC particles (Khatib, 2016). MK is renowned for the favourable effect it has on improving concrete performance, which is achieved by reacting with available calcium hydroxide/portlandite to produce secondary calcium silica hydrate (C–S–H) and various other hydrates (C_4AH_{13}, C_3AH_6 and C_2ASH_8 or Stratlingite) (Zeljkovic, 2009). This discovery has also been noted in Sabir et al. (2001) and Gruber et al. (2001).

It has been well documented that the cement hydration process and microstructure properties directly influence the chloride resistance performance of concrete. Previous studies performed by Maes et al. (2012) and Li et al. (2015) have shown that MK improves concrete's resistance to chloride attack through the refinement of the pore structure, production of C–S–H from pozzolanic reactions and the development of Friedel's salt ($3CaO{\cdot}Al_2O_3{\cdot}CaCl_2{\cdot}10H_2O$). This makes the concrete more impermeable and reduces the rate of corrosion of the steel reinforcement. Therefore, this experimental study aims to investigate the engineering properties (fresh state, mechanical and durability) of concrete incorporating MK as a supplementary cementitious material. The overall goal is towards combatting chloride attack in coastal/marine concrete structures.

2. Materials and methodology

2.1. Methodology: assessment of the effect of chloride attack on concrete

The impact of chloride attack on the concrete microstructure was assessed by following the methodology illustrated graphically in Fig. 1. The experimental approach involves first obtaining a concrete sample from a coastal area. The authors determined that it was more viable to acquire an existing concrete specimen that had been exposed to a chloride-laden environment for a long period. Hence, the concrete samples were obtained from Maydon Wharf in Durban Harbour. The climate in Durban is often described as subtropical and humid, with significantly higher volumes of precipitation in comparison with other regions of South Africa (Alexander, 2016). Research on the theoretical approach indicated that the water temperature along the Durban coast ranges from 18 to 27 °C (Alexander, 2016). The rate of chloride attack increases when concrete is situated in warm climates and exposed to saline seawater (Tadayon et al., 2016). The pictorial views of the obtained concrete samples are presented in Figs. 2 and 3. From the figures, it can be seen that the samples were subjected to tidal conditions. It was also noted that the specimens displayed signs of weathering and deterioration, which can be attributed to exposure to cyclic wetting and drying.

2.2. Methodology: assessment of the feasibility of metakaolin as an alternate binder system for concrete marine structures

The experimental approach also consists of an assessment of the feasibility of MK as an alternate binder system in concrete marine structures. As outlined in Fig. 4, this takes the form of an experimental investigation of the compression, flexural, durability and microstructure properties of concrete containing MK.

2.3. Materials

The binding agents used for this experimental investigation were Ordinary Portland Cement (OPC) and metakaolin (MK). The OPC was produced by Natal Portland Cement and classified as CEM II/B–S 42.5N Plus, which is indicative of Portland-slag cement and is in compliance with the quality and strength requirements in SANS 50197–1. Kaolin Group provided the MK used in this study (K40 High Reactive Metakaolin). The chemical composition and physical analysis of the MK have been provided in Tables 1 and 2.

The particle distribution and Scanning Electron Microscope (SEM) particle image are presented in Figs. 5 and 6. Fig. 6 shows that the MK particles are angular and platy with some degree of roughness, also noted on the surface of the MK particles. The particle shape possibly indicates that MK will improve the strength and durability performance of concrete, which can be attributed to the filler effect, the dilution effect (physical effect) and the pozzolanic reaction of MK with $Ca(OH)_2$ (chemical effect) forming additional C–S–H gel (Khater, 2010).

The fine aggregate used for this research work was Umgeni River Sand, which conformed with the constraints outlined in SANS 1083. Based on the results obtained from the sieve analysis of the fine aggregate, the fineness modulus was determined to be 2.30. The particle size distribution of the fine aggregate is represented in Fig. 7.

Coedmore Quartz Stone, with a nominal size of 19 mm, was the selected coarse aggregate for the experimental investigation. The coarse aggregate satisfied the requirements specified in SANS 1083 and was pre-graded. Potable water was used during the mixing and curing stages of the experimental study. The quality of the mixing water conforms to

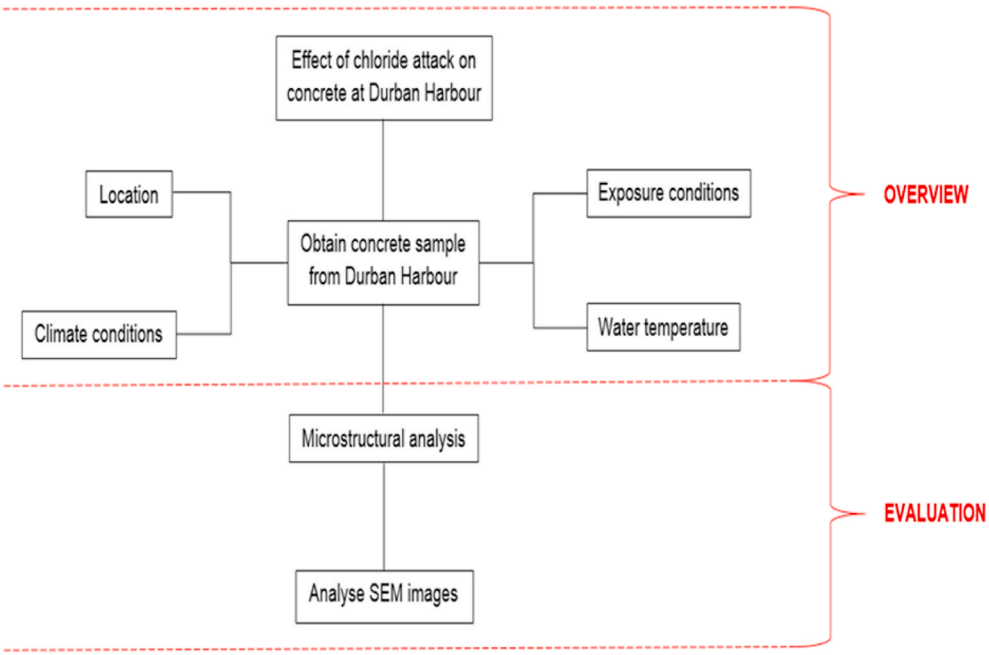

Fig. 1. Methodological processes used to determine the effect of chloride attack at the concrete sample.

Fig. 2. Location of the concrete sample obtained from Durban Harbour (Maydon Wharf).

Fig. 3. Weathering and deterioration visible on the surface of the concrete samples obtained from Durban Harbour (Maydon Wharf).

the specifications in SANS 51008.

2.4. Concrete mix design

Concrete mix designs containing 0%, 5%, 10%, 15% and 20% metakaolin (MK) as a replacement (by mass) for Portland Cement were used for the experimental investigations. The C&CI design method was used, and the mix proportions are summarised in Table 3.

2.5. Production and storage of specimens

The concrete specimens used in the experimental investigations were produced and stored according to SANS 5861–3. The concrete mixes were produced by first mixing all the dry materials (stone, sand, cement and MK) in a tilting drum mixer for 1 min, before adding water and mixing until a uniform consistency, colour and texture was achieved. The concrete was allowed to stand, while the slump and temperature were measured, followed by another 1-min mixing cycle.

After the slump and temperature of the mix were determined, the cube (150 x 150 × 150 mm) and beam (100 x 100 × 500 mm) moulds were filled and placed on a vibrating table before they were finished with a trowel. Twenty-four hours later, the specimens were demoulded and cured under normal conditions for six days. The beams were moist cured under a damp sack until 28 days, while the cubes remained in the curing bath until the 28-day strength tests. The remaining cubes were removed from the curing bath and placed under a damp sack until the 56-day strength tests. This was done to observe the effect of the different curing conditions on the strength results.

2.6. Testing procedures

The type of test, the concrete age, concrete state, mode of test and the standards/specifications considered in the experimental investigation are summarised in Table 4. The compressive strength was determined using cube tests, whereby three 150 mm concrete cubes were crushed between two platens in a hydraulic press, with a uniform loading rate of 0.3 MPa/s ± 0.1 MPa/s (Afrisam, 2018). The flexural strength was quantified by applying two loads at third points along the span of 100 x 100 × 500 mm concrete beams until flexural failure occurs. The

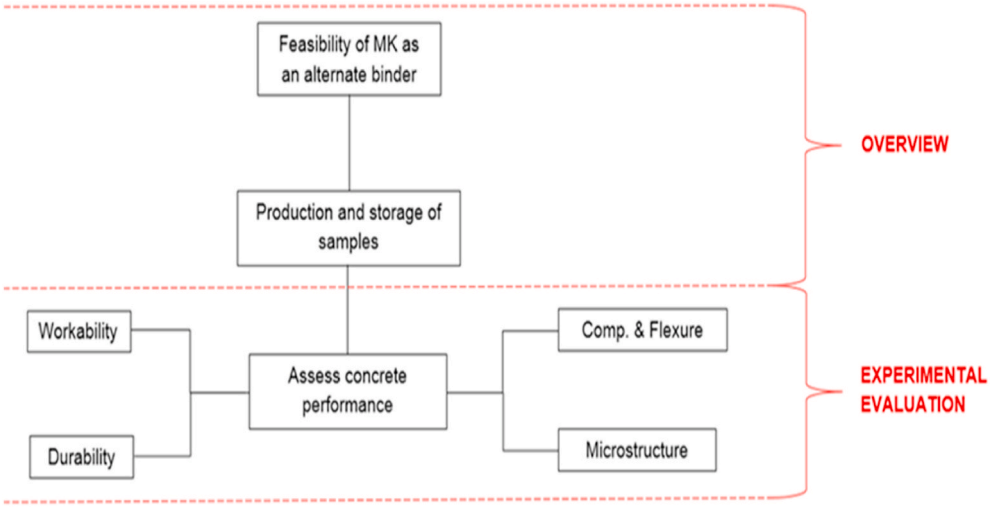

Fig. 4. Methodological processes used to assess the feasibility of metakaolin as an alternate binder system.

Table 1
Chemical analysis of K40 High Reactive Metakaolin (Kaolin Group, 2018).

Chemical	Composition (%)
SiO_2	56.8
Al_2O_2	43.5
K_2O	0.1
TiO_2	1.3
Fe_3O_2	0.5

Table 2
Physical analysis of K40 High Reactive Metakaolin (Kaolin Group, 2018).

Physical Attribute	Value
Colour	Light off-white
Whiteness	90%
Aerated powder density	320 kg/m3
Tapped powder density	390 kg/m3
Pozzolanic reactivity	± 1,000 mg Ca(OH)2/g (via Chapelle test)
BET surface area	70 m2/g
Mean particle size	d50 = 19 μm (top cut: d90 = 57 μm)

workability of the fresh state concrete was determined using the slump test. The microstructural analysis was performed using a Zeiss Leo 1450 SEM at an accelerating voltage of 5 kV. The durability of the concrete specimens was determined using the water sorptivity and porosity test; and the air and water permeability test, which are described below.

2.6.1. Water sorptivity and porosity test

The water sorptivity and porosity test were done using concrete core samples, that were obtained by cutting Ø70 mm cores from concrete cubes. An epoxy coating was applied to the sides of the cores before 30 mm thick slices were cut using a wet cutting diamond blade saw. The slices were placed in the oven to dry and removed 24 h later to allow for cooling. A calcium hydroxide solution (3g of $Ca(OH)_2$ per 1 L of tap water) was poured into a plastic tray. The dry mass of the slices was recorded before the specimens were placed on perspex strips in the calcium hydroxide solution. The stopwatch was started once the exposed face of the first slice was placed on the perspex strips. The saturated mass of the specimens was measured at 3, 5, 7, 9, 12, 16, 20- and 25-min intervals. This involved dabbing the bottom of each individual slice with a damp paper towel when it was removed from the calcium hydroxide solution. Once the saturated mass was noted, the specimen was placed back in the $Ca(OH)_2$ solution. After the 25-min interval was passed, all samples were removed from the calcium hydroxide solution. Some of the samples were left to soak in a desiccator for two days. The samples were then removed, and the mass was recorded. It was found that there was a 1,98% increase in the mass of the selected specimens. The sorptivity (S) is estimated as the slope of the line fitted between cumulative absorption values and the square root of time as given expressed by Equations (1) and (2) (Yang et al., 2019).

$$V = \frac{\Delta m}{\rho A} \tag{1}$$

$$V = S\sqrt{t} \tag{2}$$

where Δm is the mass of absorbed water. A is the area of the surface which has contact with water. t is the time of water penetration. ρ is the density of water. V is the volume of absorbed water per unit cross-sectional area.

According to Yang et al. (2019), the sorptivity and the capillary coefficient are theoretically related by the effective porosity of the concrete (Equations (3) and (4))

$$x = k\sqrt{t} \tag{3}$$

$$\varphi = \frac{S}{k} \tag{4}$$

where x is the distance of water uptake (m). k is the capillary coefficient ($m/s^{1/2}$), and φ is the porosity.

2.6.2. Air and water permeability test

Before commencing with the air and water permeability tests, a test hole (Ø10 mm and depth 40 mm) was drilled in the concrete samples. The dust resulting from the drilling process was removed, and a silicon rubber plug was inserted into the hole. The plastic screw insert was fastened into the silicon rubber plug until a tight, sealed fit was achieved. The plastic expander was then attached to the plug, and a hypodermic needle was inserted through the hole situated in the plastic expander. For the air permeability test, the vacuum tube assembly was connected to the vacuum input nozzle on the front panel of the porosiscope unit. The air tube was then attached to the air filter (prevents concrete dust particles from entering the air tube), which was in turn connected to the needle. The vacuum was pumped until both LED lights on the front panel was illuminated (i.e. the vacuum was in excess of −55 kPa). The vacuum valve was closed, and the air was filtered in to reduce the pressure to −55 kPa, at which point the left LED switched off, and the timer commenced. When the vacuum reached −50 kPa below

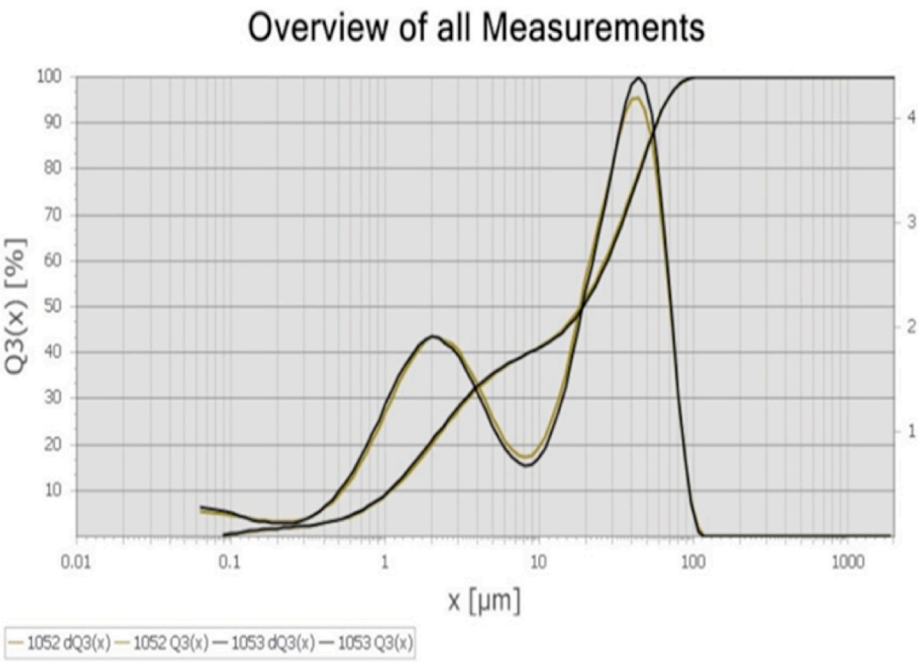

Fig. 5. Particle distribution of K40 High Reactive Metakaolin (Kaolin Group, 2018).

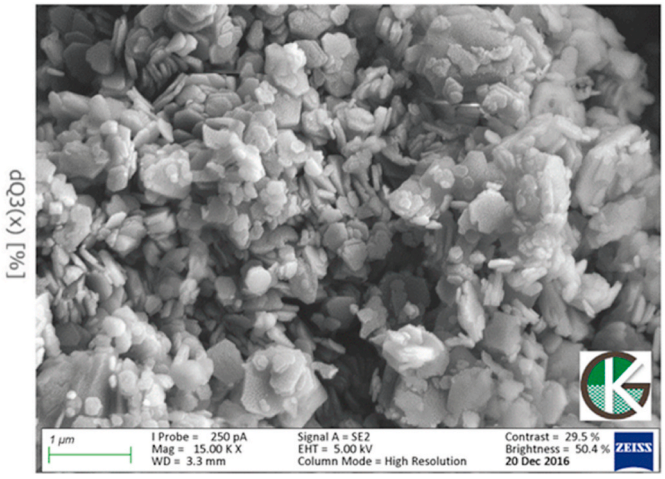

Fig. 6. Scanning Electron Microscope (SEM) particle image of K40 High Reactive Metakaolin (Kaolin Group, 2018).

atmospheric pressure, the right LED also switched off, and the timer was stopped. The time was recorded and compared with the values in Table 5, to determine the concrete category and protective quality.

The water permeability test was also performed using a porosiscope. The hypodermic needle used in the air permeability test was removed from the concrete sample, before being cleaned and re-inserted for the water permeability test. The water tube line located on top of the porosiscope unit was then connected to the needle. After attaching a stopcock to the syringe, the stopcock was opened, and the syringe was filled with tap water (±20 °C). The plunger of the syringe was depressed until the test hole was filled with water. The meniscus of the water in the nylon capillary tube was manipulated until it fell near the overflow water line situated on the outside of the porosiscope unit.

Both LED lights were illuminated, and the timer was reset when the stopcock was closed. The left LED switched off, and the timer commenced once the meniscus passed the first sensor in the porosiscope unit. When 0.01 ml of water had escaped from the concrete sample, the right LED also switched off, and the timer was stopped. Similarly, to the air permeability test, the time was recorded and compared with the specifications in Table 5, to establish the concrete category and protective quality.

3. Results and discussion

3.1. Microstructure analysis

3.1.1. Concrete sample from Durban Harbour

The SEM images obtained from the microstructural analysis of the concrete samples obtained from Durban Harbour has been presented in Fig. 8 – 11. From Figs. 8 and 9, it can be determined that there are large areas of capillary voids present in the microstructure of the concrete specimens exposed to a chloride-laden environment. These voids have detrimental effects on concrete situated in a coastal/marine setting, due to seawater entering the substructure which leads to the propagation of chloride attack and deterioration of the hydrated cement paste (HCP) and interfacial transition zone (ITZ). Concrete strength and durability are usually associated with the solids present in the HCP, whereas voids have an adverse effect on the strength and permeability characteristics.

Fig. 10 depicts the presence of microcracks on the surface of the sample from Durban Harbour. The occurrence of microcracks is dependent on the w/c ratio, cement content, level of compaction of fresh concrete, curing conditions, environmental conditions, size and grade of aggregates (Mehta and Monteiro, 2001). The formation of microcracks in the concrete sample can be attributed to the humid environmental conditions present in Durban, whereby the HCP begins to lose water which leads to drying shrinkage and the formation of cracks. This ultimately leads to deterioration of the HCP, chloride ingress and corrosion of the embedded reinforcement. According to Mehta and Monteiro (2001), the reduction of the disjoining pressure that is created by adsorbed water in the HCP structure results in drying shrinkage of concrete. The manifestation of microcracks on concrete structures can have detrimental effects on the strength and durability performance of coastal/marine structures in the Durban Harbour, as the rate of formation of microcracks is accelerated once the structure undergoes loading.

Fig. 11 indicates the existence of chemical deterioration and weathering of the surface and microstructure of the concrete sample.

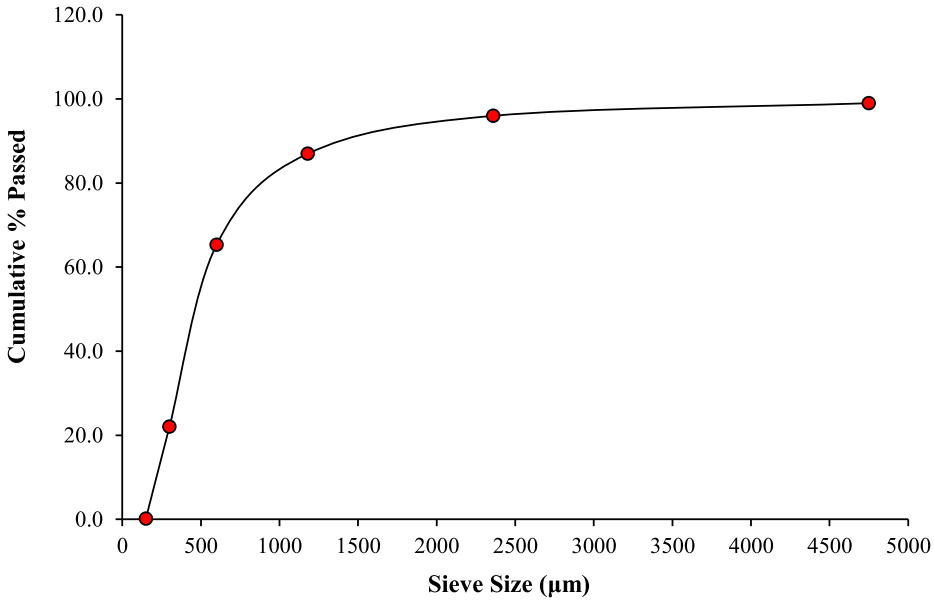

Fig. 7. Particle size distribution of fine aggregate.

Table 3
Concrete mix proportions used for the experimental investigations.

Mix	w/b	Water (l)	Binder (kg)		Stone (kg)	Sand (kg)
			OPC	MK		
0% MK	0.54	19	35	0	101	59
5% MK	0.54	19	33	1.8	101	58
10% MK	0.57	20.5	32	4	101	60
15% MK	0.58	20.5	30	5	101	58
20% MK	0.61	21.5	28	7	101	67

Table 4
Summary and details of the testing methods and specifications.

Type of test	Standard/ specification	Concrete State	Age	Mode of test
Compressive strength	SANS 5860, 5861–2, 5861–3 & 5863	Hardened state	7, 28 & 56 days	Destructive
Flexural strength	SANS 5864	Hardened state	7, 28 & 56 days	Destructive
Workability	SANS 5862-1	Fresh state	0 days (mixing stage)	Non-destructive
Durability	SANS 3001	Hardened state	28 days	Non-destructive
Microstructure	–	Hardened state	≥ 28 days	Non-destructive

Table 5
Specifications for the air and water permeability test (James Instruments, 2018)

Concrete Category	Protective Quality	Air	Permeability	Water
		Time (s)	AER* Value (s/ml)	Absorption Rate 10^3 (sec/ml)
0	Poor	<30	<8	<3
1	Not Very Good	30–100	8–25	3–10
2	Fair	100–300	25–75	10–30
3	Good	300-1,000	75–250	30–100
4	Excellent	>1,000	>250	>100

*Air Exclusion Rating

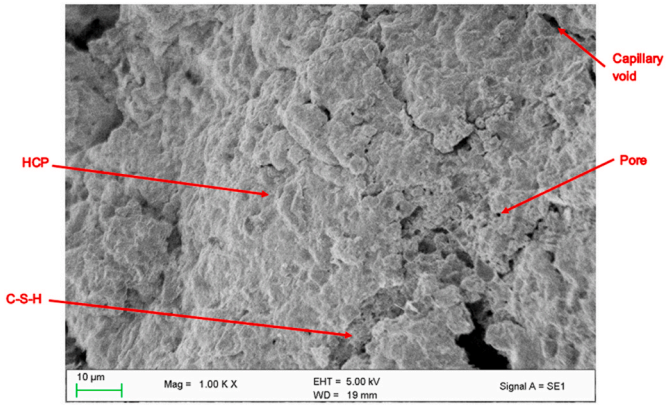

Fig. 8. SEM image of concrete sample from Durban Harbour (1).

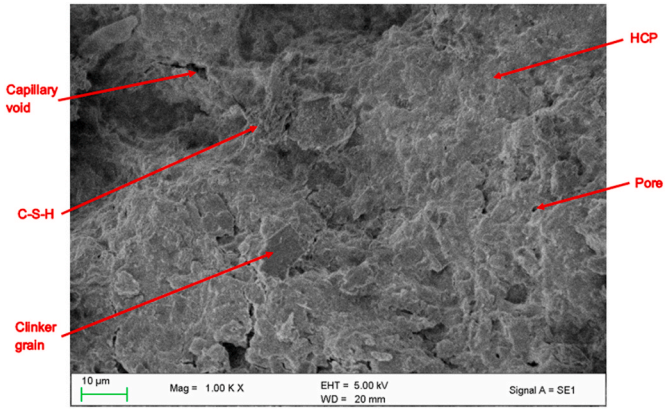

Fig. 9. SEM image of concrete sample from Durban Harbour (2).

The authors noted that the forms of degradation that were visible included: abrasion, erosion, and spalling. The level of abrasion and erosion present in the samples was particularly severe, whereby stones were protruding through the HCP. This was expected because the concrete specimens were subjected to cyclic wetting and drying resulting

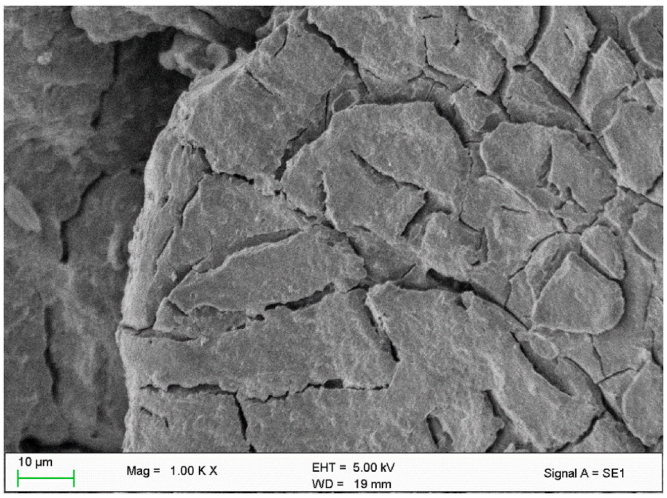

Fig. 10. Presence of microcracks and capillary voids in sample from Durban Harbour.

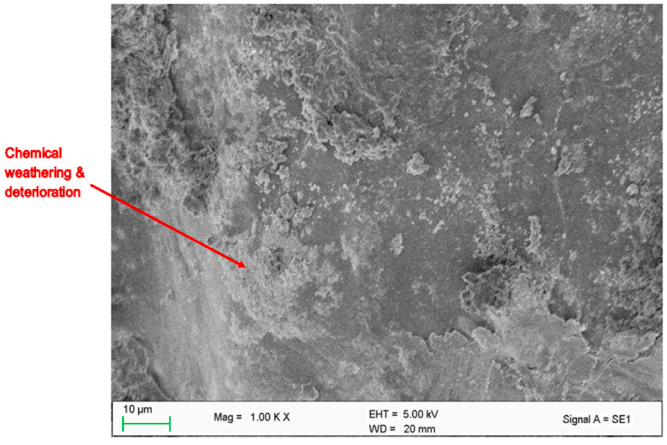

Fig. 11. Chemical weathering and deterioration of the concrete surface.

from exposure to tidal actions.

3.1.2. *Concrete samples containing metakaolin*

The results obtained from the SEM analysis of the concrete samples containing MK is presented in Figs. 12–16. It can be seen that there is a significant number of large particles present which can be classified as unhydrated clinker grains. These particles are associated with the hydration process, whereby the small clinker grains are dissolved before the larger grains (Mehta and Monteiro, 2001). It was also found that

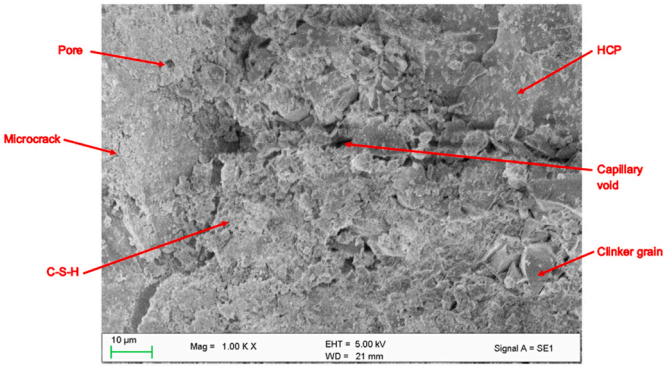

Fig. 12. SEM image of 0% MK sample.

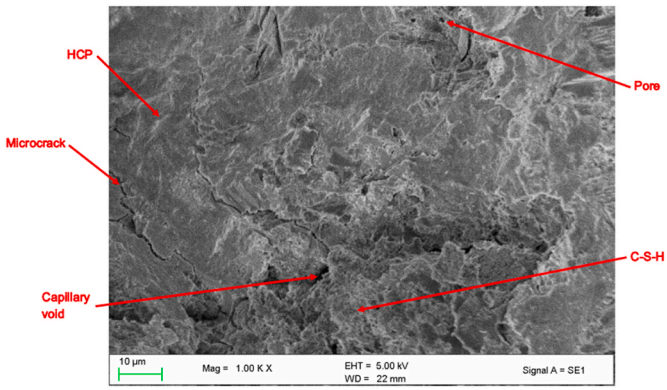

Fig. 13. SEM image of 5% MK sample.

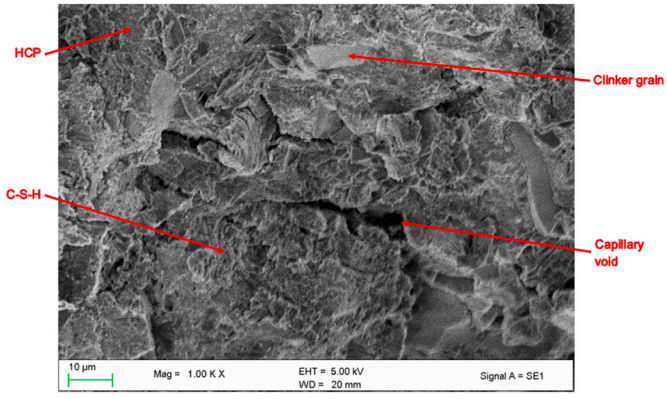

Fig. 14. SEM image of 10% MK sample.

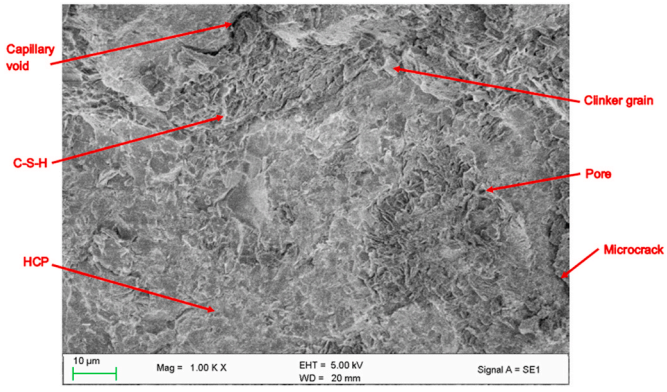

Fig. 15. SEM image of 15% MK sample.

there were various microcracks, irregularly shaped capillary voids and spherical pores present in the microstructure of the concrete specimens. The occurrence of the above-mentioned sub-structures has an adverse effect on the strength and permeability properties of concrete. It is worth noting that the size and manifestation of the microcracks, capillary voids and pores are decreasing as the MK content increases. This can be attributed to the effect of MK has improved the pore structure of concrete, by filling the voids between the cement particles, and is in line with the microstructural results obtained by Li et al. (2015).

Calcium silicate hydrate (C–S–H) constitutes a large portion of the hydrated cement paste (HCP) structure of all the samples that were analysed using electron microscopy. C–S–H consists of a microstructure that varies between crystalline fibres and a reticular network (Mehta and Monteiro, 2001). From the SEM images, it was found that the

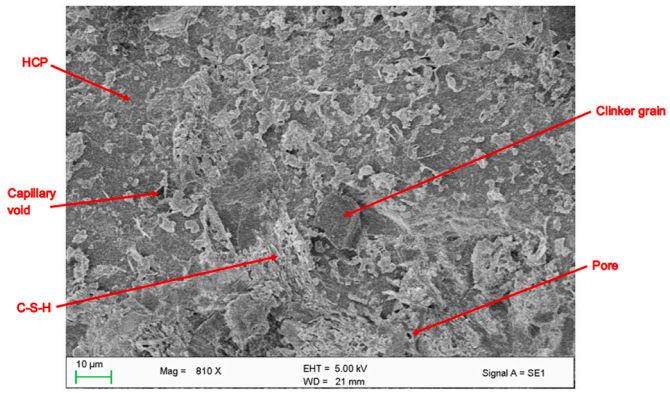

Fig. 16. SEM image of 20% MK sample.

volume of C–S–H present increases proportionally with the percentage of Portland Cement replacement with MK. This was anticipated and can be associated with the pozzolanic reactions occurring between MK and calcium hydroxide, which ultimately produces concrete with improved strength and durability properties.

3.2. Workability

The original slump was measured for the initial mix design, which was designed with a w/b ratio of 0.54. The mix proportions had to be adjusted to achieve a favourable slump, as indicated by the adjusted slump column in Fig. 17. It can be noted that the measured slump decreases as the MK content increases (Fig. 17). This indicates that the workability of the concrete mix is reduced when the percentage replacement of Portland Cement with MK increases. Jagtap et al. (2017) attributed this trend of results to the reduced fineness modulus of MK, which results in a limited amount of cement paste present to provide the lubricating effect per unit surface area of aggregate.

3.3. Temperature

The fresh state temperature reading for each mix has been detailed in Fig. 18. It can be seen that temperature decreases as the amount of MK increases. This can be attributed to the increased water levels resulting from an increase in the percentage replacement of MK.

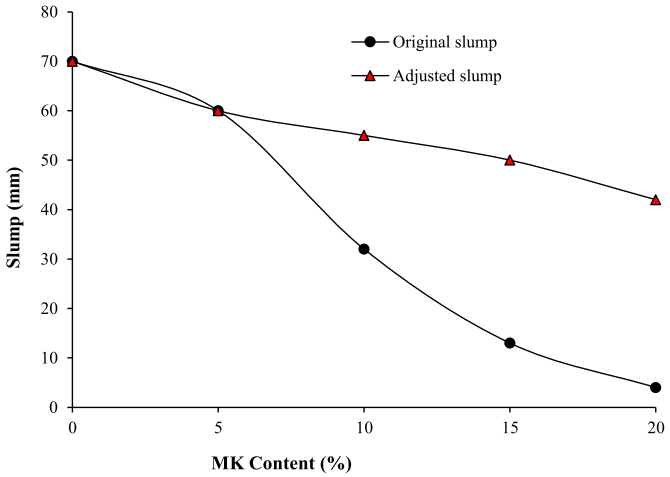

Fig. 17. Results obtained from the slump test.

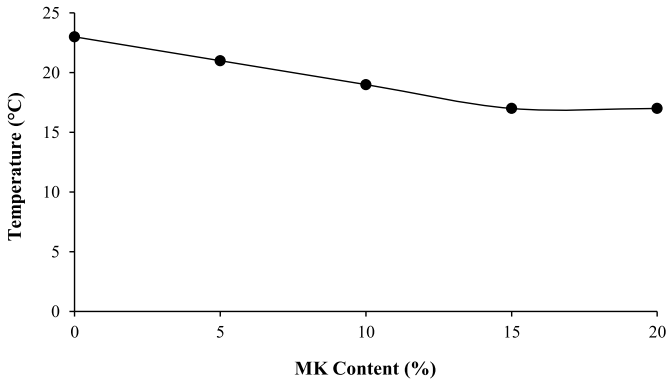

Fig. 18. Results obtained from temperature test.

3.4. Mechanical properties

3.4.1. Compressive strength

The results obtained from the 7, 28- and 56-day compressive strength tests have been graphically represented in Fig. 19. From the results, it can be seen that the compressive strength of all samples increased with time. Evidently, this was so because sufficient curing and temperature conditions were provided for the duration of the testing period. The strength gain between the 28- and 56-day tests is minor and can be attributed to the change in curing conditions outlined in Section 2. Generally, the addition of metakaolin (MK) to the concrete mix resulted in improved compressive strengths. This is attributed to the pozzolanic reaction between MK and calcium hydroxide or portlandite to produce calcium silica hydrate (C–S–H) gel, along with the formation of Friedel's salts (Khater, 2010).

However, it is worth mentioning that the 7-day compression strengths for the 5% MK mix (22.49 MPa) and the 20% MK mix (19.69 MPa) lie below the respective 7-day compression strength of the control mix (0% MK). The 20% MK mix had a higher w/b ratio (0.61) than the control mix (0.54), which is in agreement with the results obtained by Justice et al. (2005) whereby the compressive strength of samples containing MK decreased as the w/b ratio increased.

Possible reasons for the 7-day compression strength of the 5% MK mix falling below that of the control mix includes unreliable equipment, human error and the varying water level in the curing bath which results in some areas of the specimen displaying a higher strength gain when compared to other areas. The 56-day compressive strengths of the 15 and 20% MK samples also lies below that of the 0% MK samples, which can be attributed to the inflated w/b ratios of the above-mentioned samples (0.58 and 0.61).

The 10% MK mix produced the highest 7-day and 56-day compressive strength, while the 5% MK mix yielded the highest 28-day compressive strength. This is in line with the results achieved in previous studies, whereby the highest compressive strength generally occurs between 5 and 15% replacement of Portland Cement with MK. From Fig. 19, it can be concluded that the K40 High Reactive Metakaolin has a variable effect on the short term (7 day) strength and improves the long term (28 and 56 day) strength significantly.

3.4.2. Flexural strength

The flexural strength results attained from the 7, 28- and 56-day flexural strength tests have been represented in Fig. 20. Similarly, to the compression strength, it can be seen that the flexural strength of all samples improved with time. This was anticipated as an adequate curing and temperature setting was provided. Based on the results obtained, the 7-day flexural strength increases as the MK content increases, which can be explained by the production of C–S–H from pozzolanic reactions and reduction of chloride attack through the development of Friedel's salt (Li et al., 2015).

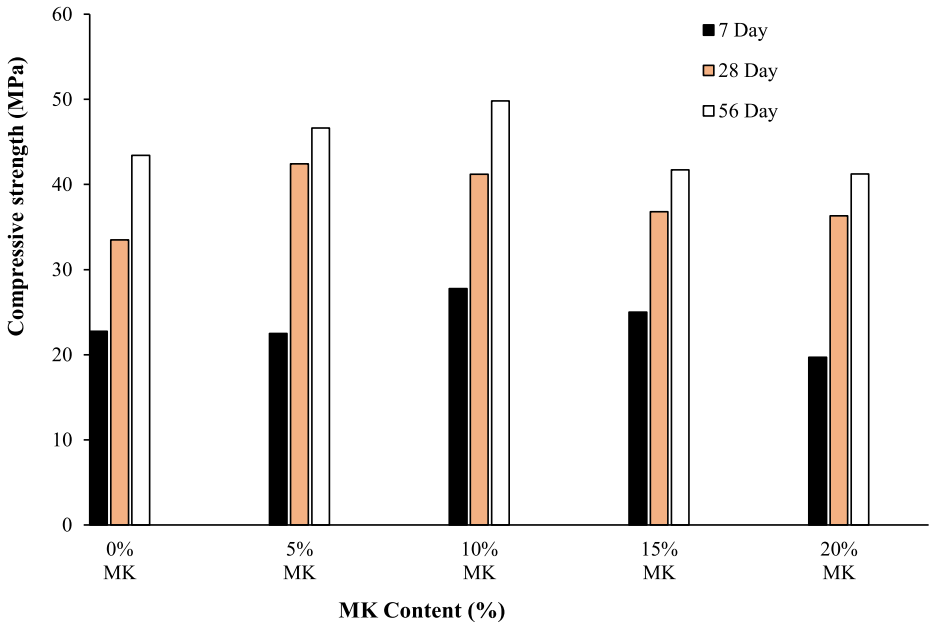

Fig. 19. Compressive strength results (7, 28 & 56 day).

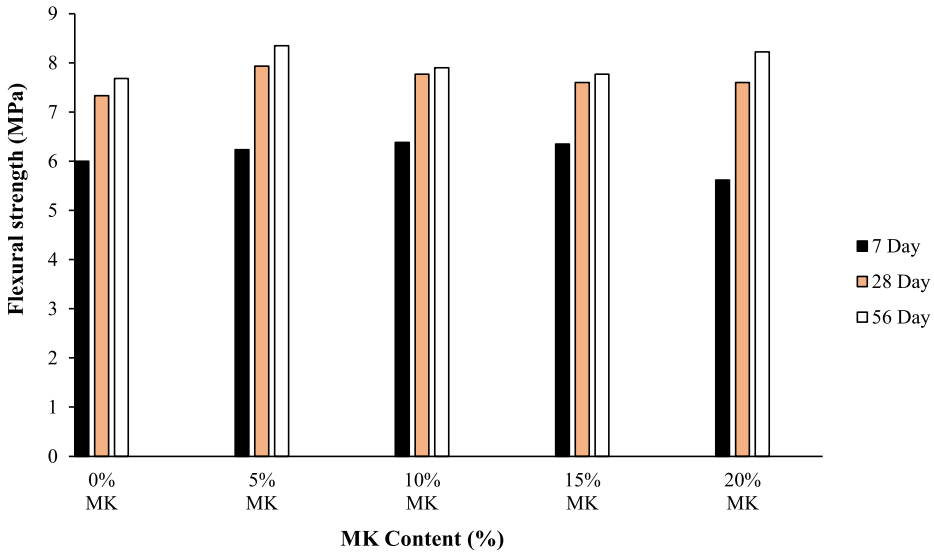

Fig. 20. Flexural strength results (7, 28 & 56 day).

However, this observation is not applicable to the 7-day flexural strength of the 20% MK mix, as it lies below that of the control mix (i.e. 0% MK). This could be attributed to the higher w/b ratio present in the 20% MK mix, which agrees with the results obtained by Justice et al. (2005). In this experimental investigation, it was found that the flexural strength decreased as the w/b ratio increased. This is due to the sufficient amount of water that is available for the hydration reaction (Justice et al., 2005).

From Fig. 20, it can be seen that all mixes containing MK have higher 28- and 56-day flexural strengths in comparison with the respective 0% MK mix. The 10% MK mix yielded the highest 7-day flexural strength, whereas the 5% MK mix produced the highest 28- and 56-day flexural strength. There is a 0.76 MPa (6.38–5.62), 0.6 MPa (7.93–7.33) and 0.67 MPa (8.35–7.68) difference between the highest and lowest respective 7, 28 and 56-day flexural strength, which indicates that there is minimal standard deviation and variance present in the flexural strength results. This could be because the concrete beam samples were removed from the curing bath after 7 days and were moist cured under a damp sack until 28 and 56 days. Based on the results represented in Fig. 20, it can be concluded that MK has a marginal effect in improving the short- and long-term flexural strength of concrete.

3.5. *Water sorptivity and porosity*

The water sorptivity and porosity test were conducted on four cylindrical slices per concrete mix, and the average mass results for each mix at the various time intervals have been graphically represented in Fig. 21. From the results obtained, the 0% MK samples had the highest average dry mass (at 0 min) and saturated mass (3–25 min), whereas the 15% MK specimens recorded the lowest dry and saturated masses.

From Table 6, the average effective porosity and water sorptivity decrease in specimens containing MK, when compared to the control mix. The 10% MK mix achieved the lowest average water sorptivity results, while the 15% MK samples displaying the lowest average

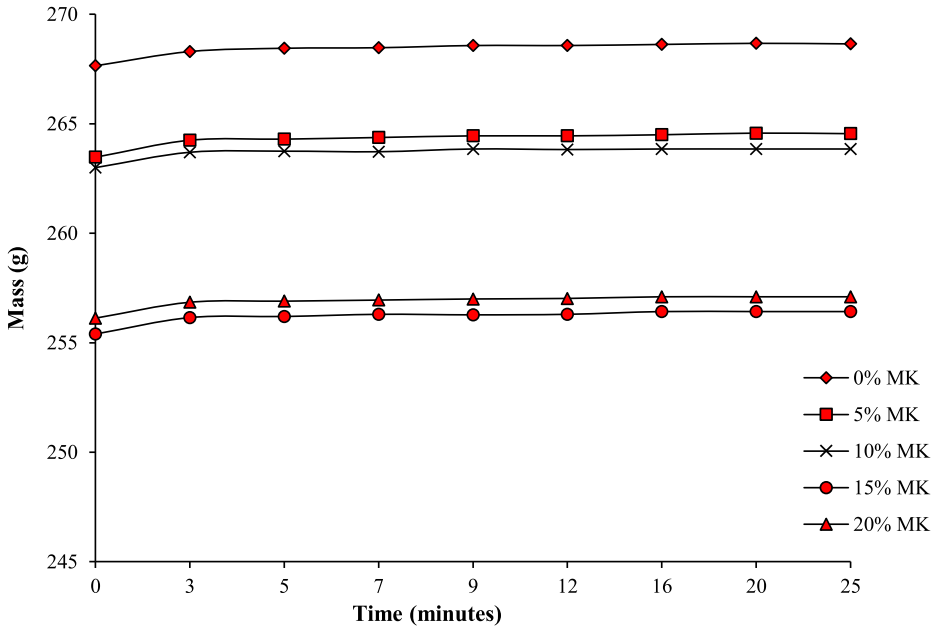

Fig. 21. Average mass results from water sorptivity and porosity test.

Table 6
Average effective porosity and water sorptivity results for concrete samples containing metakaolin.

MK Content (%)	Average effective porosity (n)	Average water sorptivity
0	0.0464	4.86
5	0.0457	4.45
10	0.0456	2.26
15	0.0443	3.57
20	0.0444	3.79

effective porosity. The filling ability of MK in cementitious matrix pores is majorly responsible for the moderate porosity and water sorptivity of the concrete (Maes et al., 2012; Li et al., 2015).

Numerous past research studies have proved that MK improves durability by reducing the permeability through the refinement of the pore structure. MK used as an alternate binder fills the void spaces between the cement particles to produce a more impermeable concrete structure (Narmatha and Felixkala, 2016). This is in line with the results outlined above, whereby the samples containing MK produced water sorptivity and porosity results that lie below that of the 0% MK specimens.

3.6. Air and water permeability

Table 7 presents the results obtained, including the time (t) taken for a vacuum reduction from −55 kPa to −50kPa (for the air permeability test) and the time taken for 0.01 ml of water to escape from the sample (for the water permeability test). For the air and water permeability tests, the protective quality improved as the MK content increased in the concrete samples. It was determined that the 10, 15 and 20% MK specimens provided excellent air permeability protection, whereas all the samples containing MK returned good protective quality results with respect to water permeability. It was found that the Water Absorption Rate (WAR) improved as the MK content increased, which is not in agreement with the results obtained from the water sorptivity and porosity test where the 10% MK and 15% MK samples produced the lowest respective water sorptivity index and average effective porosity. Possible reasons for this include human error when conducting the experimental procedure and unreliable equipment.

The favourable results can be attributed to the improved pore structure often found in concrete containing MK and is a result of MK filling the voids found between the cement particles. Khater (2010) also attributes this to the filler effect, the dilution effect (physical effect) and the pozzolanic reaction of MK with $Ca(OH)_2$ (chemical effect) which leads to the formation of additional C–S–H.

4. Conclusion

This experimental investigation examined the effect of chloride attack on concrete structures situated in a coastal/marine environment. This was achieved through a microstructural analysis of concrete samples that were obtained from the Durban Harbour (coastal area) and had been subjected to chloride attack. From the resulting analysis, it was found that the samples displayed high levels of deterioration, weathering and microcracks. This is indicative of the detrimental effect chloride attack on the strength, durability and serviceability properties of concrete structures located in the coastal environment.

Table 7
Results obtained from the air and water permeability tests.

MK Content (%)	Air Permeability				Water Permeability			
	Time (s)	AER (s/ml)	Concrete Category	Protective Quality	Time (s)	WAR (s/ml)	Concrete Category	Protective Quality
0	217	53.60	2	Fair	227	22,700	2	Fair
5	857	211.68	3	Good	493	49,300	3	Good
10	>1,000[a]	>250	4	Excellent	560	56,000	3	Good
15	>1,000[a]	>250	4	Excellent	589	58,900	3	Good
20	>1,000[a]	>250	4	Excellent	619	61,900	3	Good

[a] The precise time was not measured, as the maximum protective quality had already been achieved, hence the timer was stopped once 1,000 s had been reached.

Another key component of this study is the experimental investigation of the engineering properties (fresh state, mechanical and durability) of concrete incorporating metakaolin (MK) as supplementary cementitious material, towards combatting chloride attack in coastal/marine concrete structures. Previous studies have pointed towards improved strength and durability properties associated with concrete containing MK. This was in good agreement with the results obtained from this experimental study, where it was found that MK had a significant effect on the long-term compressive strength and a marginal effect on the flexural strength. It was also found that MK improved the pore structure of concrete, as indicated by the results obtained from the durability and electron microscopy tests. The SEM analysis showed that the microstructure of the Portland cement samples contained a high occurrence of capillary voids, which is undesirable for concrete durability performance. Alternatively, the samples containing MK displayed a more cohesive matrix, with large extents of C–S–H gels present, which is responsible for preventing the ingress of chloride ions.

Along with improvements to the mechanical performance, MK also enhanced the fresh state, aesthetic, and sustainability properties of concrete. This is attributed to the fact that the MK production process does not generate carbon dioxide CO_2 emission and requires lower temperatures when compared with the production of Portland cement (Zeljkovic, 2009). Based on these results, it can be concluded that MK is a feasible option as an alternate binder system for combatting chloride attack in concrete structures situated at coastal/marine environ.

The deterioration of concrete coastal/marine structures has an adverse effect on the safety, economy, and sustainability aspects of everyday life (Kaolin Group, 2018). A large economic and environmental burden is encountered, due to the increased amount of concrete being produced to repair and rehabilitate chloride deteriorated concrete, instead of being used in new construction projects. This burden can be eased by improving our understanding of the long-term durability factors of coastal/marine structures and incorporating MK into concrete exposed to a coastal/marine setting. This will help to save money and resources for the lifespan of the structure, while also improving the serviceability state of marine structures.

The following recommendations can be considered for future studies:

- The effect of chloride-induced corrosion in reinforced concrete can be investigated using experimental procedures such as chloride conductivity test, chloride ponding test, linear polarisation resistance (LPR) test and Tafel plot method.
- Since MK is still a relatively new cementitious material in the South African concrete industry, additional experimental investigations can be conducted to assess the viability of MK for use in concrete applications that are exposed to aggressive environments.
- Superplasticisers and water reducers can be incorporated into the concrete mix designs, to improve the workability and keep the w/b ratio consistent in all mixes. This will have a positive impact on the results acquired and enables a more accurate comparison of the results obtained for the various samples.
- A finer MK can be used to improve the compressive strength results; however, this will have a marginal effect on the permeability properties. Alternatively, a coarser MK can be implemented to produce more impermeable concrete.
- The concrete samples containing MK that were used in this study can be exposed to a chloride-laden environment to give a true reflection of the feasibility of MK in combatting chloride attack.

Ethics approval and consent to participate

This article does not contain any studies with human participants or animals performed by any of the authors.

Consent for publication

Authors give full consent to publish this research article.

Availability of data and materials

The datasets generated during the current study are available from the corresponding author on request.

Funding

The authors did not receive support from any organization for the submitted work.

Authors' contributions

DL. Pillay, MW. Kiliswa and OB. Olalusi – conceptualization, methodology & analysis, discussion, supervision, validation, writing-original draft preparation and software. PO. Awoyera, JT. Kolawole and AJ. Babafemi – methodology, discussion and writing-review.

Research involving human participants and/or animals

This article does not contain any studies with human participants or animals performed by any of the authors.

Informed consent

Not Applicable (as the results of studies does not involve any human or animal).

Declaration of competing interest

The authors declare that they have no known competing financial interests or personal relationships that could have appeared to influence the work reported in this paper.

References

Afrisam, 2018. Properties of Hardened Concrete. Technical Reference Guide, pp. 98–131.
Aguirre-Guerrero, A.M., de Gutiérrez, R.M., 2018. Assessment of corrosion protection methods for reinforced concrete. Eco-efficient Repair and Rehabilitation of Concrete Infrastructures.
Ayub, T., Shafiq, N., Khan, S., 2013. Durability of concrete with different mineral admixtures: a review. Int. J. Civ. Environ. Eng. 7 (8).
Broomfield, J., 2007. Corrosion of Steel in Concrete. Taylor & Francis, London.
Chalee, W., Jaturapitakkul, C.A., Chindaprasirt, P., 2009. Predicting the chloride penetration of fly ash concrete in seawater. Mar. Struct. 22 (3), 341–353.
Gruber, K.A., Ramlochan, T., Boddy, A., Hooton, R.D., Thomas, M.D.A., 2001. Increasing concrete durability with high-reactivity metakaolin. Cement Concr. Compos. 23 (6), 479–484.
Jagtap, S.A., Shirsath, M.N., Karpe, S.L., 2017. Effect of metakaolin on the properties of concrete. Int. Res. J. Eng. Technol. 4 (7), 643–645.
James, Instruments, 2018. Operator's Manual for C-P-6000, C-P-6050 Porosiscope.
Justice, J.M., Kennison, L.H., Mohr, B.J., Beckwith, S.L., McCormick, L.E., Wiggins, B., Zhang, Z.Z., Kurtis, K.E., 2005. Comparison of two metakaolins and a silica fume used as supplementary cementitious materials. In: Seventh International Symposium on Utilisation of High-Strength/High Performance Concrete, vols. 1&2.
Kaolin Group, 2018. Data Sheet – Metakaolin KG-K40.
Khan, M.U., Ahmad, S., Al-Gahtani, H.J., 2017. Chloride-Induced Corrosion of Steel in Concrete: an Overview on Chloride Diffusion and Prediction of Corrosion Initiation Time, vol. 2017. International Journal of Corrosion, pp. 1–9.
Khater, H.M., 2010. Influence of metakaolin on resistivity of cement mortar to magnesium chloride solution. Ceramics 54 (4), 325–333.
Khatib, J.M., 2016. Sustainability of Construction Materials, second ed. Woodhead Publishing, Duxford.
Li, Q., Geng, H., Huang, Y., Shui, Z., 2015. Chloride resistance of concrete with metakaolin addition and seawater mixing: a comparative study. Construct. Build. Mater. 101, 184–192.
Maes, M., Gruyaert, E., De Belie, N., 2012. Resistance of concrete against combined attack of chlorides and sulphates. Inter. Congress Durability Concrete.
Mehta, P.K., Monteiro, P.J.M., 2001. Concrete: Microstructure, Properties and Materials.
Narmatha, M., Felixkala, D., 2016. Meta kaolin –the best material for replacement of cement in concrete. IOSR J. Mech. Civ. Eng. 13, 66–71, 04.

Owens, G., 2013. Fundamentals of Concrete, third ed. The Concrete Institute, Midrand, South Africa.
respeAlexander, M.G., 2016. Marine Concrete Structures: Design, Durability and Performance. Elsevier Science, Kent.
Sabir, B., Wild, S., Bai, J., 2001. Metakaolin and calcined clays as pozzolans for concrete: a review. Cement Concr. Compos. 23 (6), 441–454.
Schneider, M., 2019. The cement industry on the way to a low-carbon future. Cement Concr. Res. 124, 105792.
Singh, N.B., Middendorf, B., 2020. Geopolymers as an alternative to Portland cement: an overview. Construct. Build. Mater. 237, 117455.
Song, H.W., Lee, C.H., Ann, K.Y., 2008. Factors influencing chloride transport in concrete structures exposed to marine environments. Cement Concr. Compos. 30 (2), 113–121.
Tadayon, M.H., Shekarchi, M., Tadayon, M., 2016. Long-term field study of chloride ingress in concretes containing pozzolans exposed to severe marine tidal zone. Construct. Build. Mater. 123, 611–616.
Tamanna, K., Raman, S.N., Jamil, M., Hamid, R., 2020. Utilisation of wood waste ash in construction technology: a review. Construct. Build. Mater. 237, 117654.
Yang, L., Gao, D., Zhang, Y., Tang, J., Li, Y., 2019. Relationship between sorptivity and capillary coefficient for water absorption of cement-based materials: theory analysis and experiment. R. Soc. Open Sci. 6 (6), 190112.
Zeljkovic, M., 2009. Metakaolin Effects on Concrete Durability. Masters. University of Toronto.